POAC'13
Espoo, Finland

Proceedings of the 22nd International Conference on
Port and Ocean Engineering under Arctic Conditions
June 9-13, 2013
Espoo, Finland

STATIC FRICTION OF ICE

Erland M. Schulson and Andrew L. Fortt
Ice Research Laboratory, Thayer School of Engineering, Dartmouth College,
Hanover, NH 03755 USA

ABSTRACT

Slide-hold-slide experiments on first-year sea ice and fresh-water ice have established that holding opposing surfaces under stress at -10 ^{o} C and at -30 ^{o} C for periods up to 10^4 s raises the resistance to sliding by as much as a factor of three or more. The effect is termed static strengthening and is modelled in terms of creep and fracture of asperities that protrude from opposing surfaces and interact at points of contact.

1. INTRODUCTION

Consider a sheet of sea ice loaded by wind and ocean current and sliding, either over itself through rafting, as illustrated in Figure 1a, or against itself along through-thickness cracks and faults within the cover, as illustrated in Figure 1b. Experiments designed to simulate this behavior have shown that for sliding at a constant velocity V, shear resistance τ is set by the compressive stress σ_n applied normal to the interface and by the coefficient of kinetic friction μ_k, through Coulomb's relationship $\tau = \tau_o + \mu_k \sigma_n$ where τ_o may be viewed as a measure of cohesive strength. Under conditions relevant to the Arctic $\tau_o \sim 0$ and the friction coefficient varies from μ_k ~0.4 to 1.6, depending on velocity and temperature (Fortt and Schulson, 2011; Lishman et al. 2011). The friction coefficient exhibits velocity strengthening at lower speeds and velocity weakening at higher speeds, effects that are attributed, respectively, to creep deformation at points of contact across the sliding interface and to a combination of fracture and localized melting (Fortt and Schulson, 2011). Accompanying sliding is the generation of heat (Golding et al., 2010).

Should sliding be interrupted for a period of time, owing say to a reduction in wind forcing, what would be the magnitude of the shear stress required to reinitiate sliding? Would it be greater then the stress required to maintain sliding at the previous velocity? If so, by how much? And why? Questions of this kind, of course, are not limited to ice on cold oceans, but arise also in relation to frictional shearing and attendant heating across cracks and faults within the icy crust of tectonically active bodies within the outer solar system, such as Jupiter's Europa (Tufts et al., 1999; Hoppa et al., 2000; Nimmo and Gaidos, 2002; Dombard and McKinnon, 2006) and Saturn's Enceladus (Nimmo et al., 2007; Smith-Konter and Pappalardo, 2008; Olgin et al., 2011).

To explore these points, we are currently performing systematic slide-hold-slide (SHS) experiments in the laboratory on first-year sea ice and, for reference, on fresh-water ice. In this paper we show that holding under load can have a significant effect on the coefficient of static friction, as noted earlier by Lishman et al. (2011) and Sukhorukov et al. (2012), and we describe a model of the effect in terms of the geometry and deformation of asperities that

protrude from opposing interface and interact at points of contact. We also comment briefly on the applicability of our findings to situations in nature. A more complete account of the work may be found elsewhere (Schulson and Fortt, 2013).

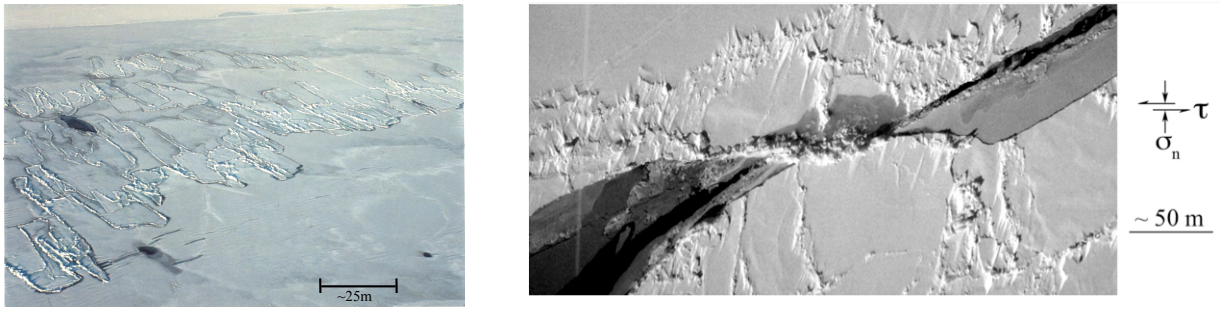

(a) (b)

Figure 1. Photographs of (a) rafts and (b)sliding cracks within a first-year sea ice cover on the Beaufort Sea.

2. EXPERIMENTAL PROCEDURE

The sea ice of the study had been harvested during the winter of 2009 from the ice cover on the Beaufort Sea, at 71°N, 156°W, and stored in the Ice Research Laboratory at Dartmouth. The ice was comprised of columnar-shaped grains of 6.1±2.3 mm column diameter and possessed the S2 growth texture. Its melt-water salinity was 4-5 ppt and its density (at -10 °C) was 918±4 kg m^{-3} at -10 °C. The fresh-water ice was produced in the laboratory, as described elsewhere (Golding et al., 2010), in the form of equiaxed and randomly oriented aggregates of grains 1.5±0.5 mm diameter of density (at -10 °C) 909.9±4.2 kg m^{-3}, termed granular ice. Specimens of both kinds of ice were milled in the form of pads (41 × 41 × 23 mm^3) and sliders (76 × 46 × 25 mm^3) were attached to mounts within a double-shear device of stiffness 2.0±0.5 MN m^{-1}. The device and cooling chamber, shown in Figure 2, are fully described elsewhere (Schulson and Fortt, 2012). The roughness of the sliding surfaces was R_a=0.76±0.51 for the sea ice and R_a= 0.43±0.24 μm for the granular ice, measured using a calibrated Surtronic 25 profilometer. The sliding surfaces of the sea ice were cut parallel to the long axis of the columnar grains and sliding across them was imposed in a direction perpendicular to the columns. Most of the experiments described here were performed at -10 °C, at sliding velocities from V_s=10^{-6} to 10^{-4} m s^{-1}, imposed by a servo-hydraulic actuator that is part of the double-shear device. A few tests were performed on sea ice at -30 °C at V_s=10^{-6} m s^{-1}. All tests were run under an applied normal stress of $\sigma_n = 60$ kPa.

The SHS tests were performed as follows. Following a period of steady-state sliding at a constant velocity V_s, during which the frictional shear stress τ reached a constant level, albeit marked by oscillations related to slip-stick behavior, sliding was stopped for a period of time by stopping the actuator. During that period, the normal stress across the interface was maintained constant, at the level set during sliding. Subsequently, the actuator was re-activated at the initial velocity and sliding eventually resumed, initially at a velocity greater than the pre-holding speed but shortly thereafter at the pre-holding velocity. Post-hold-sliding was continued until steady state was again established. Shortly thereafter, sliding was stopped and the interface was allowed to rest under normal stress for a greater period of time before sliding was re-initiated. The holding/healing period t_h was varied from t_h=1 to 10^4 s. Most tests were performed in triplicate.

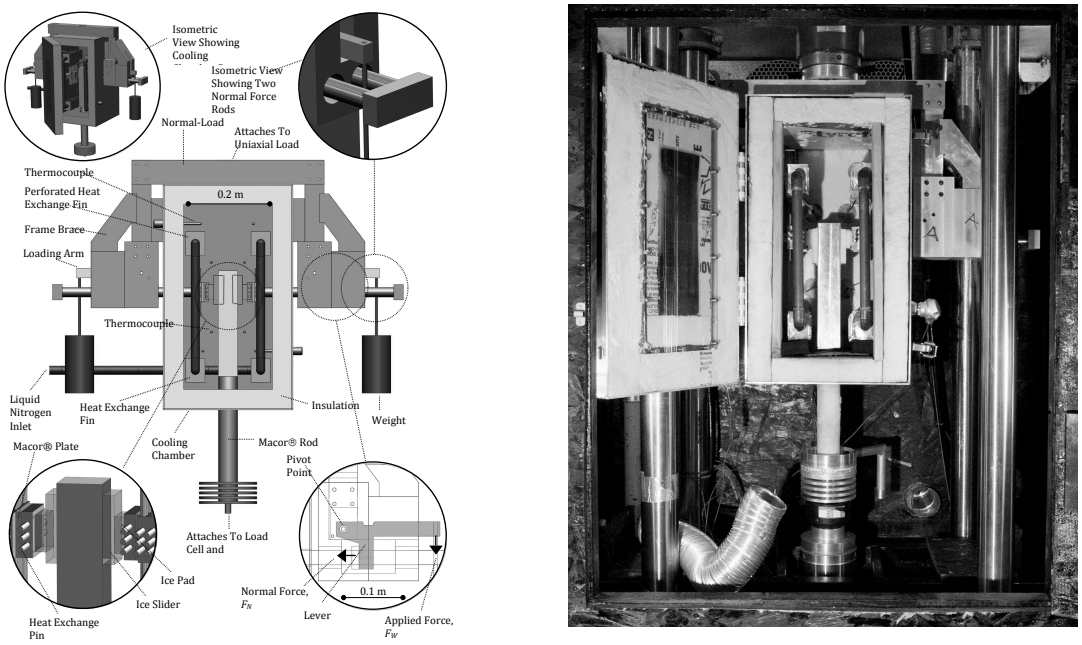

a) b)

Figure 2. (a) Drawing and (b) photograph of cooling chamber and double-shear device.

3. RESULTS

Figure 3 shows a series of SHS curves generated by sliding at -10 ^{o} C. The curves are presented in terms of the stress ratio τ / σ_n vs. displacement. The inserts show expanded views after holding 100 seconds. For both kinds of ice after each hold period (noted on the plots) the stress ratio increased, but returned quickly (i.e., over a sliding distance of a few tens of micrometers) to essentially the pre-holding steady-state value once sliding was resumed. For the purpose of this discussion, we take the maximum stress ratio to be the coefficient of static friction, $\mu_s = (\tau / \sigma_n)_{\max}$; we take the steady-state ratio to be the coefficient of kinetic friction, $\mu_k = (\tau / \sigma_n)_{ss}$.

Figure 4 shows graphs of μ_s vs. $\log t_h$, derived from Fig.3. Note that the coefficients of static and kinetic friction are essentially equal for very short hold times, but then static friction increases. We term the difference between the two coefficients "static strengthening"; i.e., $\Delta\mu = \mu_s - \mu_k$. Static strengthening:

(i) is first detected once holding exceeds a threshold period t_t that decreases with increasing velocity, from $t_t \sim 30$ s at $V_s = 10^{-6}$ m s^{-1} to $t_t \sim 3$ s at $V_s = 10^{-5}$ m s^{-1} to (upon extrapolating) $t_t \sim 0.3$ s at $V_s = 10^{-4}$ m s^{-1};

(ii) increases approximately logarithmically with time, scaling as $\Delta\mu \propto \beta \log_{10} t_h$ for $t_t < t_h < t_u$ where the strengthening coefficient $\beta = 0.30 \pm 0.03$ is independent of velocity and where t_u denotes an upper limit to logarithmic dependence;

(iii) increases with increasing velocity, and when viewed in terms of the product $V_s t_h$, scales approximately linearly with $\beta \log_{10}(V_s t_h)$ for $t_t < t_h < t_u$, Figure 5;

(iv) may be described also by the power law $\Delta\mu \propto t_h^m$, Figure 6, where the exponent has the value $m \sim 0.5 \pm 0.10$ over the range $t_t < t_h < t_u$;

(v) exhibits little thermal sensitivity over the range -10 ^{o}C to -30 ^{o}C, Figure 7, at least in sea ice sliding slowly; and

(vi) exhibits little sensitivity to the salinity in sea ice, reminiscent of the insensitivity to this factor of the coefficient of kinetic friction (Kennedy et al., 2000; Fortt and Schulson, 2011).

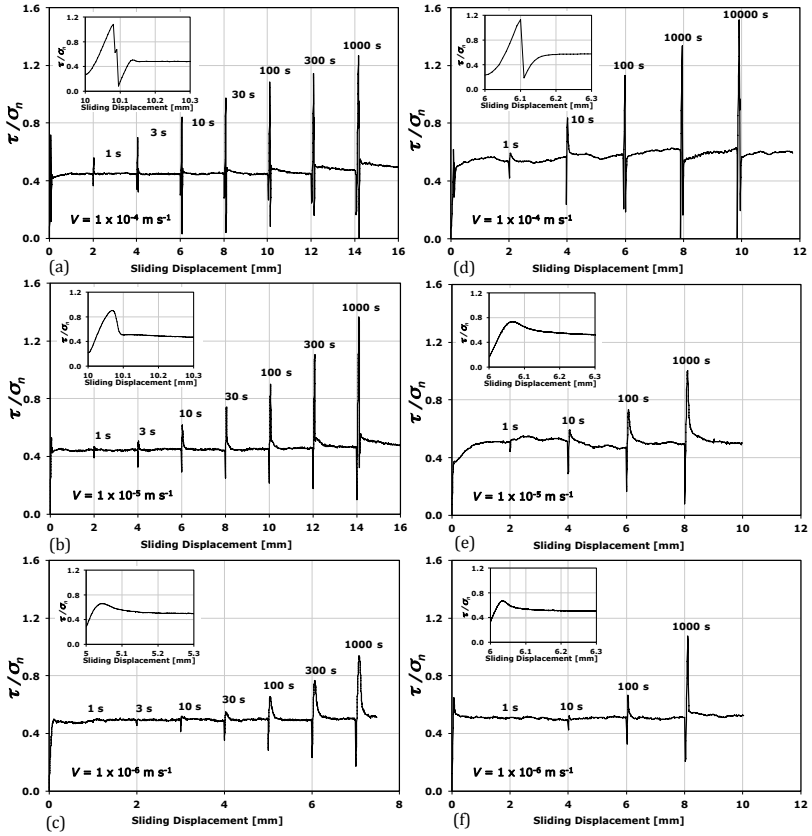

Figure 3. Plots of frictional shear stress (τ) divided by normal stress (σ_n) vs. displacement from SHS tests at -10 ^{o} C on first-year sea ice (a-c) and fresh-water granular ice (d-f) at actuator velocities of 10^{-6}, 10^{-5} and 10^{-4} m s^{-1}. The inserts show expanded segments of re-loading at the same velocity after holding 100 seconds.

Static strengthening is not unique to ice. It has been observed for a variety of other materials, including rock (Dieterich, 1978; Marone, 1998), metals (Dokos, 1946) and glassy polymers (Berthoud et al., 1999). There, too, it is characterized by logarithmic dependence on holding time. The difference is that in those cases the strengthening coefficient β is lower than it is for warm ice by about an order of magnitude, owing presumably to lower homologous temperatures during testing.

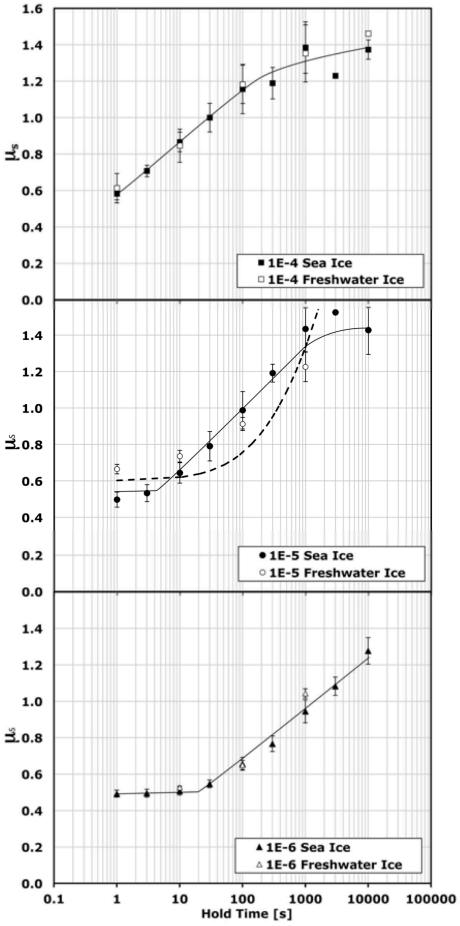

Figure 4. Plots of the coefficient of static friction vs. log holding time from SHS curves of the kind shown in Fig.3. The bars through the averages denote standard deviations. The dashed line on the middle plot was calculated using Equation 7.

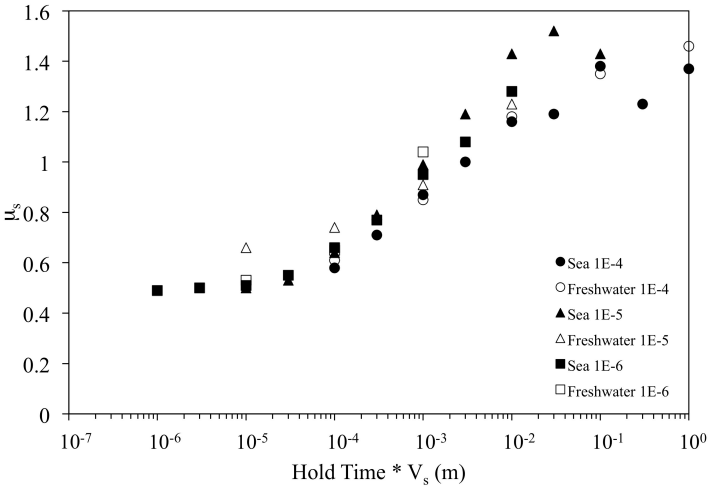

Figure 5. From the averages shown in Fig.4, plots of the coefficient of static friction vs. the $\log_{10}$ of the product of hold time and actuator velocitv.

4. DISCUSSION

We account for this behavior in terms of the mechanical interaction of asperities that protrude from opposing surfaces.

The interaction time t_i is the sum of the time for contacts to slip over each other prior to holding plus the time of holding under stress; i.e.

$$t_i = a_o / V_s + t_h \qquad (1)$$

where a_o denotes the initial diameter of the contact. Holding begins to exert a detectable effect once the second term in Equation (1) equals the first term; i.e., when the threshold period of holding $t_h = t_t$ is comparable to the slip time. It follows that:

$$a_o \approx V_s t_t \,. \qquad (2)$$

Then, from the present results (Section 3 (i)) $a_o = 10^{-6} x30 = 10^{-5} x3 = 10^{-4} x0.3 = 30\mu m.$ When holding time is normalized w.r.t. threshold time, $t_h / t_t = V_s t_h / a_o$, the dependence of strengthening on the product $V_s t_h$ (Fig. 5) follows naturally.

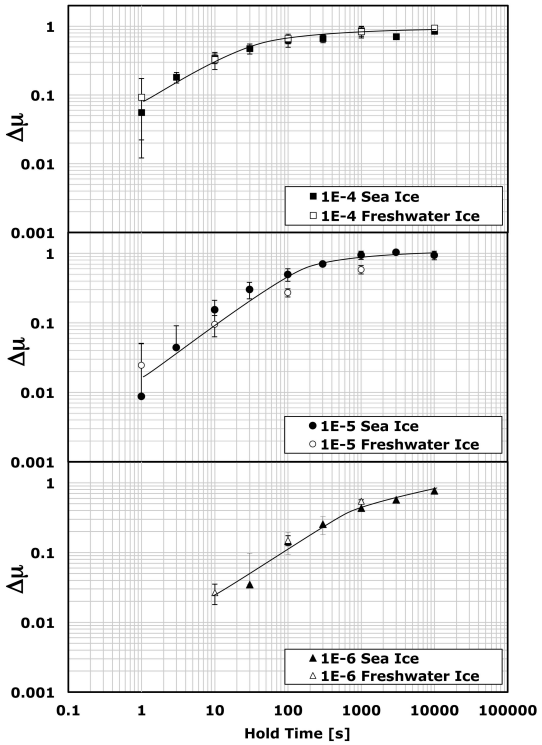

Figure 6. Plot of $\log_{10}$ static strengthening ($\Delta\mu = \mu_s - \mu_k$ where μ_s and μ_k denote the coefficients of static and kinetic friction, respectively) vs. $\log_{10}$ hold time, from the data shown in Fig.4.

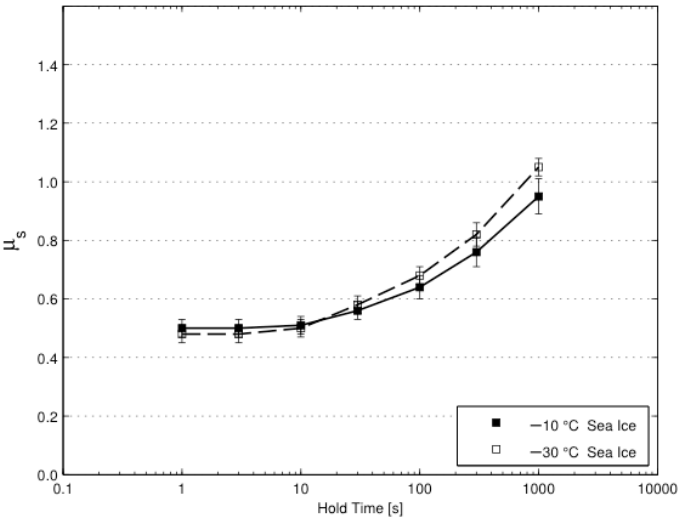

Figure 7. Plot of the coefficient of static friction for sea ice at -10 ^{o}C and at -30 ^{o} C upon holding after sliding at 10^{-6} m s^{-1}.

To estimate the number of pairs of asperities in contact *N*, we follow Bowden and Tabor (1964). Accordingly, we equate the normal stress supported by each contact to the hardness *H* of the ice and then equate the total load supported by all contacts $H\pi a_o^2 N/4$ to the applied normal load $F_n = \sigma_n A_a$ where A_a denotes the apparent area of contact. Thus:

$$N = 4\sigma_n A_a / \pi H a_o^2 . \qquad (3)$$

Taking *H*=10 to 30 MPa (Barnes et al. 1971) we obtain the estimate $5\times10^3 \le N \le 14\text{x}10^3$. Correspondingly, the areal density of contacts $\rho_A = N / A_a = 5.6\pm3.0\ \text{x}10^6$ m^{-2}, the average spacing between contacts $\lambda \sim \rho_A^{-1/2} \sim 400\mu m$, and the real contact area A_r is related to the apparent area through the relationship $A_r / A_a = \sigma_n / H$, giving $0.002 \le A_r / A_a \le 0.006$. Interestingly, the areal density derived from the above analysis is almost the same as the density $5.5\text{x}10^6$ m^{-2} measured by Hatton et al. (2009) from sliding experiments on similar material under similar conditions (S2 ice, 7.3 ppt salinity, -10^{o} C, V_s=10^{-4} m s^{-1}, σ_n =10 kPa).

Asperities creep when in contact: their height decreases and their diameter increases from a to a_o. The contact area thus increases by a factor $(a/a_o)^2$. To quantify this factor we invoke both conservation of volume $h_o a_o^2 = h a^2$ and power-law creep $\dot{\varepsilon} = B\bar{\sigma}^n$ where B is a temperature-dependent materials constant; $\bar{\sigma}$ takes into account the multiaxiality of the stress state (through a combination of compressive stress H and frictional drag $H\mu_k$) within the deforming material and is given by $\bar{\sigma} = H\left[1+3\alpha^2\mu_k^2\right]^{1/2}$ where α denotes the fractional retention of the residual shear stress within the contact (owing to stress relaxation during holding) and μ_k denotes the steady-state coefficient of kinetic friction. In so doing, we obtain the relationship (Schulson and Fortt, 2013):

$$\left(\frac{a}{a_0}\right)^2 = \left[1 + n\,BH^n\left(1+3\alpha^2\mu_k^2\right)^{\frac{n}{2}} t_h\right]^{\frac{1}{n}}. \qquad (4)$$

Appropriate parametric values (noted below) suggest areal increases as high as a factor of 5 for holding time of 10^4 s. This increase is large enough to activate microstructural changes such as dynamic recrystallization, although we have no direct evidence of this kind of transformation within contact zones.

On the coefficient of static friction μ_s, we define this parameter in the usual manner as the ratio of the shear force to re-initiate sliding after holding F_s to the applied normal force F_n; i.e.

$$\mu_s = F_s / F_n = (\tau_s / H)(a/a_o)^2 \qquad (5)$$

where τ_s denotes the shear strength of the bonded contact. Given that drag induces tension, we assume the bond strength to be limited by the tensile strength of the ice σ_t such that $\tau_s = \sqrt{\left[\sigma_t + (H/2)\right]^2 - (H/2)^2}$ under the multiaxial stress state created by the applied shear and normal loads. Thus, we can show that (Schulson and Fortt, 2013):

$$\mu_s = \left[(\sigma_t / H) + 0.5)^2 - 0.25\right]^{0.5}\left[1 + nBH^n(1+3\alpha^2\mu_k^2)^{n/2} t_h\right]^{1/n}. \qquad (6)$$

Upon insertion of parametric values appropriate to -10 ^{o} C (n=3 and B=4.3x10^{-7} MPa^{-3}s^{-1} (Barnes et al., 1971), the mid-range value H =20 MPa (Barnes et al., 1971), σ_t= 6 MPa (Schulson and Duval, 2009) and $\mu_o = 0.5$ (present result)) and assuming $\alpha = 0.5$, we obtain for the static coefficient of friction at -10 ^{o}C for $t_t < t_h < t_u$:

$$\mu_s(t_h) = 0.6\left[1 + 0.01 t_h\right]^{1/3} \qquad (7)$$

for t_h in seconds. Lessening the degree of stress relaxation by increasing from $\alpha = 0.5$ to $\alpha = 1.0$ raises the coefficient of friction by only about 10 %.

The model (Equation (7)) and measurements agree reasonably well at the intermediate velocity of 10^{-5} m s^{-1} for $t_h \le 1000$ s (dotted line, Fig.4). Under other conditions the

agreement is not as good. The model over-estimates the measurements at greater time (at 10^{-5} m s^{-1}) and it over-estimates and under-estimates the measurements, respectively, at the lowest and highest velocities, by about 20-40%. The encouraging point is that it captures, albeit imperfectly, the character of strengthening as well as the order of magnitude of the effect.

That sea ice and fresh-water ice exhibit such similar behavior may seem surprising, for it is known that in bulk form sea ice creeps more rapidly than fresh-water ice under a given set of conditions and that it possesses lower tensile strength (for review see Schulson and Duval, 2009). However, when cognizance is taken of the fact that in the form of tiny asperities sea ice is probably unaccompanied by strength-lowering pockets of brine, the similarity is less surprising.

How does the above model account for the non-detection of a significant effect of temperature on static strengthening? The parameters that depend most sensitively on temperature are hardness and the creep constant, principally through the product BH^n. These parameters vary in the opposite sense: H increases with decreasing temperature while B decreases (Barnes et al., 1971). Together, they tend to work against a large effect of temperature.

On the logarithmic dependence on time of static hardening (Fig.4), we note that that description can be obtained from an analysis similar to the one described elsewhere. Brechet and Estrin (1994) showed that by using an exponential function to describe creep instead of a power law, namely $\dot{\varepsilon} = \dot{\varepsilon}_o \exp[(h / h_o)(\sigma_y / S)]$ where $\dot{\varepsilon}_o$ is a temperature-dependent constant, σ_y denotes the yield stress and its equated hardness and S is a strain rate sensitivity parameter:

$$a^2 / a_o^2 = h_o / h = \{1 + \frac{S}{H} \ln\left[1 + \dot{\varepsilon}_o t \frac{H}{S} \exp\frac{H}{S}\right]\} \tag{8}$$

and:

$$\mu = \mu_o \{1 + \frac{S}{H} \ln\left[1 + \dot{\varepsilon}_o t \frac{H}{S} \exp\frac{H}{S}\right]\}. \tag{9}$$

Equation (9) is difficult to compare to our results because we do not have for ice independent measurements of S and of $\dot{\varepsilon}_o$.

Finally, there is the question of adhesion and the mechanism of its initiation during SHS tests. Sintering may play a role, but probably not a major one, for separate calculations of neck growth via the mechanism of vapor transport, the one most likely to dominate under the conditions of the present experiments (see Blackford (2007) for a thorough review of sintering of ice), indicate growth rates too low by an order of magnitude or more. More important may be freeze-bonding via the rapid freezing of melt water that forms through frictional heating during sliding prior to holding. In mind is not freezing of a thin layer of water of the kind that forms on the entire surface of warm ice during sliding at high velocities (>0.1 m s^{-1}, (Oksanen and Keinonen, 1982)), for calculations indicate that at the low velocities applied here the increase in surface temperature is expected to be too low to melt ice whose temperature is initially ten degrees or more below the equilibrium melting point; i.e., $\Delta T \leq 0.01$ ° C. Instead, we imagine the freezing of patches of melt-water that form perhaps from thermal flashes at localized points of contact that for a short period of time experience velocities during the slip stage of the stick-slip cycle higher than the average applied velocity. Asperities different in size from the average may also be significant.

Pressure melting-cum-freezing at contact points may help as well, but alone cannot account for adhesion because pressure comparable to the hardness of the ice lowers the equilibrium melting point only by $0.8 \leq \Delta T_{mp} \leq 2.4$ ° C. The liquid-like layer present on the surface of warm ice (for review see Dash, 2006) may also play a part, given the observation (Szabo and Schneebeli, 2007) of sub-second bonding between needles of ice when brought together under a normal load of 1 Newton at temperatures above ~ -23 ° C. The point here is that a solid-state process alone is unlikely to initiate adhesion. Instead, the freezing of a small amount of water is probably necessary.

In closing and returning to natural scenarios, we sense that static strengthening is to be expected within the relatively warm crust of ice on cold terrestrial oceans, through the operation of the same physical processes described above. Neither salinity nor temperature is expected to exert a large effect on the strength imparted. In keeping with this view are the results of Sukhorukov et al. (2012) who, from preliminary SHS tests in the field using both "wet" and "dry" meter-sized blocks, observed static strengthening upon holding for a short period (up to 80 s). Whether static strengthening plays a role as well in the relatively cold crust on cold icy satellites is less clear, although prolonged periods of holding under extraterrestrial conditions would to some extent counteract the lower creep rate of cold ice.

More work is needed.

ACKNOWLEDGEMENTS
This work was supported by NASA-Outer Planets Research, grant no.NNX09AU27G and by U.S Dept. of the Interior-BSEE, contract no. E12PC00064.

REFERENCES
Barnes, P., Tabor, D., et al. 1971. The friction and creep of polycrystalline ice. *P.R. Soc. Lond. A Mat.,* 1557**,** 127-155.
Berthoud, P., Baumberger, T., et al. 1999. Physical analysis of the state- and rate- dependent friction law: Static friction. *Phys. Rev. B,* 59**,** 14313-14327.
Blackford, J. R. 2007. Sintering and microstructure of ice: a review. *J. Phys. D Appl. Phys.,* 40**,** R 355-R 385.
Bowden, F. P. and Tabor, D. 1964. The Friction and Lubrication of Solids, Part II. Oxford, Clarendon Press.
Brechet, Y. and Estrin, Y. 1994. The effect of strain rate sensitivity on dynamic friction of metals. *Scripta Metall. Mater.,* 30**,** 1449-1454.
Dash, J. G., Rempel, A. W., et al. 2006. The physics of premelted ice and its geophysical consequences. *Rev. Mod. Phys.,* 78**,** 695-741.
Dieterich, J. H. 1978. Time-dependent friction and and the mechanics of stick-slip. *Pure Appl. Geophys.,* 116**,** 790-806.
Dokos, S. J. 1946. Sliding Friction under Extreme Pressures .1. *J. Appl. Mech.-Trans. ASME,* 13**,** A148-A156.
Dombard, A. J. and Mckinnon, W. B. 2006. Elastoviscoplastic relaxation of impact crater topography with application to Ganymede and Callisto. *J. Geophys. Res.,* 111**,** doi:10.1029/2005JE002445.
Fortt, A. and Schulson, E. M. 2011. Frictional sliding across Coulombic faults in first-year sea ice: A comparison with freshwater ice. *J. Geophys. Res.,* 116**,** 13
Golding, N., Schulson, E. M., et al. 2010. Shear faulting and localized heating in ice: The influence of confinement. *Acta Mater.,* 58**,** 5043-5056.

Hatton, D. C., Sammonds, P. R., et al. 2009. Ice internal friction: Standard theoretical perspectives on friction codified, adapted for the unusual rheology of ice, and unified. *Phil. Mag.,* 89**,** 2771-2799.
Hoppa, G. V., Greenberg, R., et al. 2000. Distribution of strike-slip faults on Europa. *J. Geophys. Res.,* 105**,** 22617-22627, doi:10.1029/1999JE001156.
Kennedy, F. E., Schulson, E. M., et al. 2000. Friction of ice on ice at low sliding velocities. *Phil. Mag. A,* 80**,** 1093-1110.
Lishman, B., Sammonds, P., et al. 2011. A rate and state friction law for saline ice. *J. Geophys. Res.,* 116.
Marone, C. 1998. The effect of loading rate on static friction and the rate of fault healing during the earthquake cycle. *Nature,* 391**,** 69-71, doi:10.1038/34157.
Nimmo, F. and Gaidos, E. 2002. Thermal consequences of strike-slip motion on Europa. *J. Geophys. Res,* 107, doi: 10.1029/2000JE001476.
Nimmo, F., Spencer, J. R., et al. 2007. Shear heating as the origin of plumes and heat flux on Enceladus. *Nature,* 447**,** 289-291, doi:10.1038/nature05783.
Oksanen, P. and Keinonen, J. 1982. The mechanism of friction of ice. *Wear,* 78**,** 315-324.
Olgin, J. G., Smith-Konter, B. R., et al. 2011. Limits of Enceladus's ice shell thickness from tidally driven tiger stripe shear failure. *Geophys. Res. Lett.,* 38, L02201, doi:10.1029/2010GL044950.
Schulson, E. M. and Duval, P. 2009. Creep and Fracture of Ice. Cambridge, Cambridge University Press, 416 pp.
Schulson, E. M. and Fortt, A. L. 2012. Friction of ice on ice. *J. Geophys. Res.,* 117.
Schulson, E.M. and Fortt, A. 2013. Static strengthening of frictional surfaces of ice. *Acta Mater.* 61, 1616-1623.
Smith-Konter, B. and Pappalardo, R. T. 2008. Tidally driven stress accumulation and shear failure of Enceladus's tiger stripes. *Icarus,* 198**,** 435-451.
Sukhorukov, S., Määttänen, M., et al. Field experiments on the friction coefficient of sea ice on sea ice. 21st IAHR Intern. Symp. on Ice, 2012. Dalian, China.
Szabo, D. and Schneebeli, M. 2007. Subsecond sintering of ice. *Appl. Phys. Lett.,* 90**,** Art. No. 151916 APR 9 2007.
Tufts, B. R., Greenberg, R., et al. 1999. Astypalaea Linea: A Large-Scale Strike-Slip Fault on Europa. *Icarus,* 141**,** 53-64.